# POWER VARIATIONS OF AN X-RAY FEL OSCILLATOR IN SATURATION*

R. R. Lindberg† and K.-J. Kim[1], Argonne National Laboratory, Lemont, IL, USA
[1]also at University of Chicago, Chicago, IL, USA

## Abstract

Basic FEL theory predicts that the fractional power fluctuations of an ideal oscillator in steady state should be given by the ratio of the spontaneous power in the oscillator bandwidth to that stored in the cavity at saturation. For the X-ray FEL oscillator with its narrow bandwidth Bragg crystal mirrors, this ratio is typically a few parts per million, but some simulations have shown evidence of power oscillations on the percent level. We show that this is not related to the well-known sideband instability, but rather is purely numerical and can be eliminated by changing the particle loading. We then briefly discuss to what extent variations in electron beam arrival time may degrade the power stability.

## INTRODUCTION

The x-ray FEL oscillation (XFELO) has the potential to be an intense source of narrow-bandwidth x-rays that is also incredibly stable [1, 2]; theory predicts that the fractional pulse-to-pulse energy stability could approach the $10^{-5}$ to $10^{-6}$ level. We investigate ways in which this stability might be disturbed, showing that the sideband instability will not be an issue, that certain power fluctuations observed in simulation are purely numerical, and the extent to which electron arrival time jitter affects FEL output.

## SIDEBAND INSTABILITY

Ideally, an FEL oscillator at saturation should operate like standard atomic lasers, outputting steady-state pulses of radiation whose energy is approximately constant and whose spectral content can approach the Fourier limit. On the other hand, there are many potential causes for variations in the saturated output power of an FEL oscillator. These include fluctuations in the cavity and/or electron beam properties, short-pulse effects that arise when the distance that the radiation of central wavelength $\lambda_1$ slips ahead of an electron after $N_u$ undulator periods becomes comparable to the electron beam duration $\sigma_e$, and instabilities. Perhaps the best-known instability is the sideband or trapped particle instablity, in which particle motion in the ponderomotive bucket during a single pass can lead to large variations in output power and multi-modal spectral output.

We can understand the physics of the sideband instability using the arguments of [3]: we consider a perturbation of the radiation power like that shown in Fig. 1(a), where the power $P_1 \sim P_{\text{sat}} = (I/e)\gamma mc^2/2N_u$, with $I$ the electron beam current, $\gamma$ the Lorentz factor, and $e$, $m$, and $c$ the electron charge, mass, and the speed of light. If the width of region 1 equals the synchrotron period in region 1 $\sim \lambda_1(P_{\text{sat}}/P_1)^{1/4} \sim N_u\lambda_1$, then in the first half of the undulator the particles in region 1 make one-half a synchrotron oscillation and lose the energy $\sim \gamma mc^2(P_1/P_{\text{sat}})^{1/4}/2N_u$ to the field. In the second half of the undulator where these particles are in the absorptive phase, the field has slipped ahead by a distance $N_u\lambda_1/2$ and the particles extract energy from the wave in region 2. On the other hand, if we consider the particles initially in region 2 we find that since the power and hence the synchrotron frequency is initially smaller, they do not make a full half-rotation in the bucket after half the undulator length. Thus, they lose less energy to region 2 than is given to region 1, and extract less energy from region 3 than particles initially in region 1 take from region 2. The net effect is that the perturbation is amplified, so that in general the FEL oscillator in saturation is unstable to the growth of sidebands at frequencies $\omega_1 \pm \omega_s \sim (2\pi c/\lambda_1)(1 \pm 1/N_u)$.
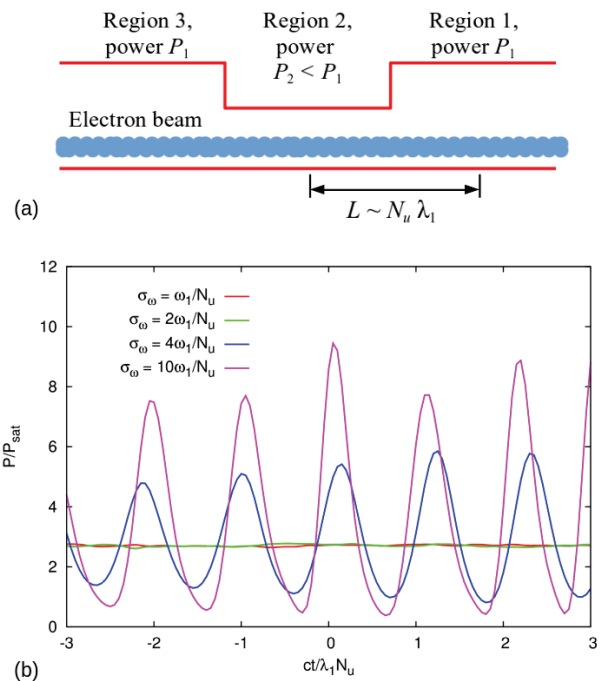


Figure 1: (a) Illustration of a perturbation that would be amplified by the sideband instability. (b) Saturated output power for various mirror bandwidths $\sigma_\omega$ that are of order the synchrotron frequency at saturation $\omega_1/N_u$.

Since the instability amplifies the sidebands at normalized frequency difference $\pm 1/N_u$, we expect that it can be suppressed in oscillators that have narrow-bandwidth reflective mirrors. For example, the x-ray FEL oscillator [1, 2]

(XFELO) uses Bragg crystal mirrors whose reflective bandwidths are less than a few times $10^{-6}$, which is much smaller than the normalized synchrotron frequency $1/N_u \gtrsim 3\times10^{-4}$, and we expect that the XFELO is largely immune to the sideband instability. To investigate this further, we ran a number of extended 1D simulations as described in [4], in which we (artificially) varied the bandwidth of the crystal mirror. For this study we assume that the reflectivity is Gaussian with width $\sigma_\omega$, so that it acts on the field in frequency space via the multiplication by $\sqrt{R}e^{-\omega^2/4\sigma_\omega^2}$, where the reflectivity $R$ is chosen to be 0.85.

We summarize the results of this study in Fig. 1(b), where we plot the power in saturation scaled by $P_{\text{sat}} = (I/e)\gamma mc^2/2N_u$ as a function of time normalized by the characteristic synchrotron period $\lambda_1 N_u/c$ for four different mirror bandwidths $\sigma_\omega$. The plot shows that the sideband instability, with its characteristic power peaks length $\sim N_u\lambda_1$, is active when the mirror bandwidth is larger than about twice the synchrotron frequency, $\sigma_\omega \gtrsim 2\omega_1/N_u$, and otherwise plays no role on the saturated dynamics. Although this precise value of $\sigma_\omega$ that is required will depend upon the cavity power $P$, which in turn depends upon the cavity gain and loss, this dependence is weak ($\sim P^{1/4}$), and will not affect an XFELO that has $\sigma_\omega/(\omega_1/N_u) \lesssim 10^{-2}$.

## SIMULATIONS OF STEADY STATE OPERATION

In the previous section we showed that the sideband instability does not plague an XFELO because of the spectral filtering provided the Bragg crystal mirrors. Hence, we expect that the steady-state power fluctuations can in principle approach the theoretical limit given by the spontaneous radiation power emitted into the narrow Bragg bandwidth. Nevertheless, some XFELO simulations have shown evidence of a long-wavelength power oscillation in saturation. We show an example in Fig. 2; (a) demonstrates the characteristic exponential growth and saturation after $\sim 200$ passes, while panel (b) plots the same thing on a linear scale, showing clear evidence in the stored energy about its mean of approximately 18 μJ. We have found that these oscillations can be correlated with periodic variations of the radiation phase that in this case occur with a period $\sim 4 \times 130$ passes. Since the FEL gain should not depend upon the radiation phase initially random particles, we suspect that the oscillations have a numerical rather than physical origin. In fact, we have found that they are due to the way in which the macroparticle phases are initialized.

The standard macroparticle loading scheme [5,6] carefully chooses the initial particle phases $\theta_j = (k_1 + k_u)z - ck_1t_j$ to correctly simulate the shot noise with a small number of particles (here $t_j$ is the particle time when it reaches location $z$ in the undulator, while $k_1 = 2\pi/\lambda_1$ and $k_u = 2\pi/\lambda_u$). To do this in the presence of non-zero energy spread and emittance, the loading scheme divides the total number of particles within any slice $N_{\text{slice}}$ into $N_{\text{slice}}/N_b$ "beamlets"
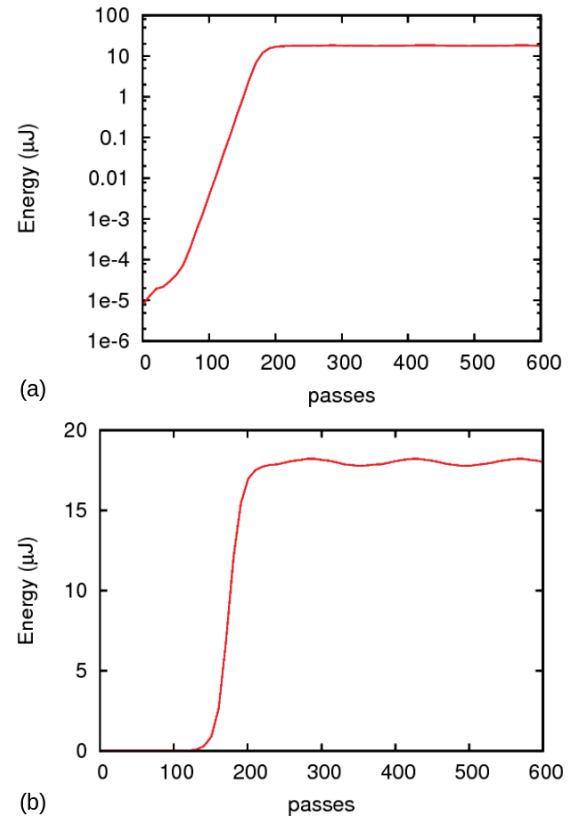


(a)



(b)

Figure 2: (a) Exponential growth of the XFELO cavity energy and subsequent saturation at pass $\sim 200$. (b) Same graph on a linear scale, which shows clear evidence power oscillations whose period is 120 passes.

with $N_b$ particles, and initializes the phase according to

$$\theta_j|_{n,\ell} = \frac{2\pi}{N_b}\left(n + \frac{N_b^2}{N_{\text{slice}}}\ell\right) + (2\delta)r_{n,\ell}, \tag{1}$$

where $1 \leq n \leq N_b$ labels the particles within a beamlet, $1 \leq \ell \leq N_{\text{slice}}/N_b$ identifies the beamlet, $r_{n,\ell}$ is a random number between 0 and 1, and $\delta \approx \sqrt{3N_{\text{slice}}/N_{\text{real}}}$ sets the initial simulation bunching statistics to match that of a electron beam that has $N_{\text{real}} \gg N_{\text{slice}}$ randomly distributed electrons; the macroparticles within a beamlet have an identical energy and transverse coordinates, which insures that the shot noise statistics is maintained even as the phase changes due to energy spread and emittance.

If the energy oscillations seen in Fig. 2 are physical, they should not depend upon the particle loading. Figure 3 tests this by varying both the number of macroparticles per slice and the number per beamlet: panel (a) uses $N_{\text{slice}} = 2048$, (b) has $N_{\text{slice}} = 4096$, while (c) uses $N_{\text{slice}} = 8192$, and we clearly see that the oscillation amplitude decreases with the number of macroparticles. More interestingly, Figure 3(a)-(b) both show that the oscillation amplitude decreases at fixed $N_{\text{slice}}$ as the number of particles per beam $N_b$ is increased, and furthermore that this increases the energy oscillation frequency. Further investigation shows that this latter effect
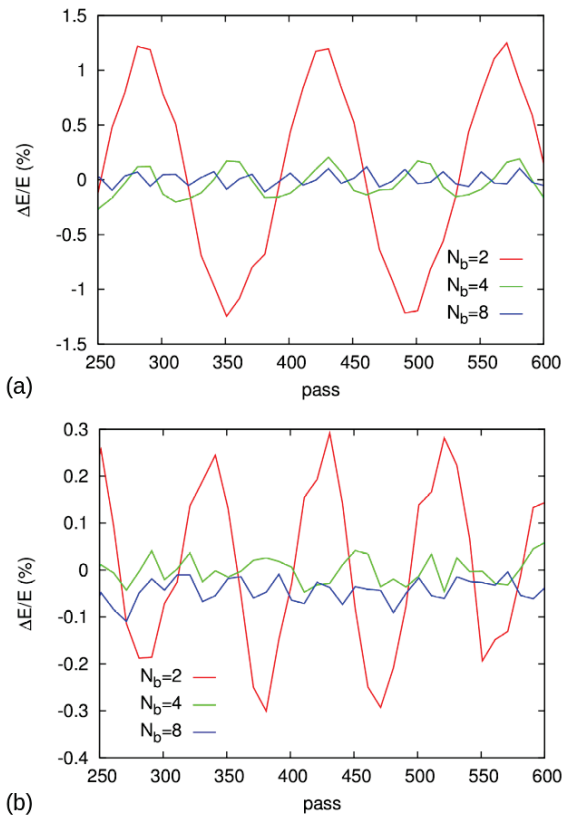
(a)

(b)

Figure 3: XFELO cavity power after saturation for (a) 2048 macroparticles/slice and (b) 4096 macroparticles/slice. The red, green, and blue lines indicate the number of particles per beamlet as described in the text, which shows that the power oscillations are numerical artifacts that depend upon the initial loading.

is related to the linear increase in the radiation phase with pass number. Since the gain depends weakly on the initial relative phase between the electrons and the field, the gain oscillates as the phase inreases. Inspection of the loading Eq. (1) indicates that for $\delta \ll 1$ the phase difference between particles and field that corresponds to a local maximum (or minimum) in the gain is when the phase changes by $2\pi/N_b$; hence, it is periodic at twice the freqnuency, and the period of the gain oscillation is roughly $2N_b$ times smaller than period of the phase change. Figure 3 clearly shows the halving of the oscillation period as $N_b$ is doubled from 2 to 4 (red and green lines); the blue line with $N_b = 8$ also follows this trend, although the precise frequency is more difficult to discern.

## VARIATIONS IN ELECTRON BEAM ARRIVAL TIME

Finally, we close by presenting some simulation results regarding how variations in the electron-beam arrival time affects FEL output. Previous work [4] has shown that reasonable XFELO gain can be maintained in the presence static timing errors whose magnitude is $\lesssim 15$ fs for the parameters listed in Table 1. The net linear gain here is about 15%, and

Table 1: XFELO Parameters for Simulations

| Name | Symbol | Value |
|---|---|---|
| Energy | $\gamma_0 mc^2$ | 7 GeV |
| Energy spread | $\sigma_\gamma/\gamma_0$ | $2 \times 10^{-4}$ |
| Normalized emittance | $\varepsilon_n$ | 0.2 mm · mrad |
| Peak current | $I$ | 10 A |
| Bunch length | $\sigma_t$ 1 ps | |
| Undulator periods | $N_u$ | 3000 |
| Undulator length | $L_u$ | 53 m |
| Rayleigh range | $Z_R$ | 10 m |

we have found that the saturated energy decreases by about 30% when the timing error $\Delta T = 10$ fs $= \sigma_t/100$. Furthermore, if the arrival time varies slowly over many passes then the cavity energy at any instant will approximately equal that of its corresponding steady-state value. In this case we expect that feedback can be usefully applied to reduce any variations.

Figure 4 considers the other extreme in which the arrival time jitter fluctuates randomly from pass to pass. Here, we assume that the arrival time is uniformly distributed between $-\Delta t$ and $\Delta t$, and Fig. 4 shows that the stored cavity energy has very small fluctuations when $\Delta T \lesssim 10$ fs $= \sigma_t/100$, while the fluctuations increase to the several percent level if $\Delta T = 50$ fs. Finally, we see that the XFELO gain is maintained and the energy fluctuations are manageable even in the presence of arrive time jitter $\sim \sigma_t/10 = 100$ fs.
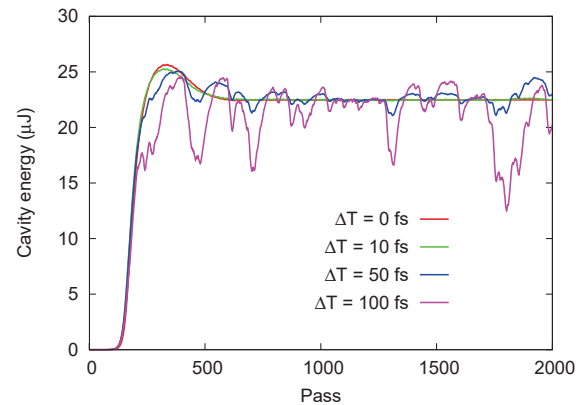


Figure 4: Stored XFELO energy for various random jitter in the arrival time, which is assumed to be a uniformly distributed random number between $-\Delta T$ and $\Delta T$.

## CONCLUSIONS

We have shown that the narrow bandwidth Bragg crystal mirrors of an XFELO effectively suppress the sideband instability. Additionally, we have found that certain particle loading schemes can lead to spurious energy fluctuations in the XFELO output, and indicated how one might avoid these. Finally we showed that the XFELO output is not strongly affected by arrival time jitter that is $\lesssim 10\%$ of the bunch length.

# REFERENCES

[1] K.-J. Kim, Y. Shvyd'ko, and S. Reiche, "A Proposal for an X-Ray Free-Electron Laser Oscillator with an Energy-Recovery Linac", *Phys. Rev. Lett.*, vol. 100, p. 244802, Jun. 2008, doi:10.1103/PhysRevLett.100.244802

[2] R. Colella and A. Luccio, "Proposal for a free electron laser in the X-ray region", *Opt. Commun.*, vol. 50, p. 41-44, May 1984, doi:10.1016/0030-4018(84)90009-9

[3] R. W. Warren, J. C. Goldstein, and B. E. Newnam, "Spiking mode olperation for a uniform-period wiggle." *Nucl. Instrum. Methods Res. Sec. A*, vol. 250, p. 19-25, Sep. 1986, doi:10.1016/0168-9002(86)90854-5

[4] R. R. Lindberg and K.-J. Kim, "Mode growth and competition in the x-ray free-electron laser oscillator start-up from noise", *Phys. Rev. ST-AB*, vol. 12, p. 070702, Jul. 2009, doi:10.1103/PhysRevSTAB.12.070702

[5] C. Penman and B. W. J. McNeil, "Simulation of input electron noise in the free-electron laser", *Opt. Commun.*, vol. 90, p. 82, Aug. 1992, doi:10.1016/0030-4018(92)90333-M

[6] W. M. Fawley, "Algorithm for loading shot noise microbunching in multidimensional, free-electron laser simulations", *Phys. Rev. ST Accel. Beams*, vol. 5, p. 070701, Jul 2002, doi:10.1103/PhysRevSTAB.5.070701